Available online at www.sciencedirect.com
ScienceDirect
Deep-Sea Research I 55 (2008) 277–295
DEEP-SEA RESEARCH PART I
www.elsevier.com/locate/dsri

Thin layers of plankton: Formation by shear and death by diffusion

Daniel A. Birch*, William R. Young, Peter J.S. Franks

Scripps Institution of Oceanography, University of California at San Diego, La Jolla, CA 92093-0213, USA

Received 22 June 2007; received in revised form 15 November 2007; accepted 19 November 2007
Available online 23 December 2007

Abstract

We show that a steady vertically-sheared current can produce a thin layer of plankton by differentially advecting an initial patch whose vertical and horizontal dimensions are H_0 and L_0, respectively. Our model treats the plankton as an inert passive tracer with vertical diffusivity κ_v and subject to a vertically-sheared horizontal current with shear α. After a transient of duration $L_0/\alpha H_0$ the vertical thickness H of the patch decreases with $H(t) \approx L_0/\alpha t$. This shear-driven thinning is halted by diffusion at a time of order $\alpha^{-2/3}\kappa_v^{-1/3}L_0^{2/3}$, and at this time the layer achieves a minimum layer thickness of order $\alpha^{-1/3}\kappa_v^{1/3}L_0^{1/3}$. For typical oceanic parameters, such as $\kappa_v \sim 10^{-5}\,m^2\,s^{-1}$, $\alpha \sim 10^{-2}\,s^{-1}$, and $L_0 \sim 1000\,m$ the initial transient is about 3 h and the layer achieves a minimum thickness of order 1 m in a time of order 1 day. During the shear thinning the intensity of the layer decreases by a factor of $3^{-1/2} \approx 0.58$, which means that the intensity of the thin layer is comparable to the intensity of the patch from which it was formed. Subsequently the layer thickens and its intensity decreases; the *coup de grace* is delivered by shear dispersion at a time of order H_0^2/κ_v. The lifetime of the thin layer, defined by the condition that the maximum concentration is comparable to the initial maximum concentration, is the same order as the time to achieve minimum thickness. Additionally, analysis of a nutrient–phytoplankton model shows that phytoplankton growing in a sheared patch of nutrients can result in a layer of phytoplankton that develops as an initially thin feature.

PACS: 92.20.Jt; 92.10.Ns; 87.23.Cc; 92.40.Cy

Keywords: Thin layers; Plankton; Finestructure; Advection–diffusion; Patchiness; Mathematical models

1. Introduction

Thin layers of phytoplankton appear to be ubiquitous features of coastal waters (Strickland, 1968; Derenbach et al., 1979; Jaffe et al., 1998; Dekshenieks et al., 2001; Johnston et al., 2008). Discovered by Strickland (1968), thin layers were first sampled in detail by Derenbach et al. (1979) using one of the earliest *in situ* fluorometers. Phytoplankton thin layers generally appear as spikes in vertical profiles of fluorescence or beam attenuation; these spikes are often many times the background intensity and have vertical scales of tens of centimeters to meters. More recently, the

*Corresponding author. Tel.: +1 858 534 1504; fax: +1 858 534 8045.
E-mail addresses: dbirch@ucsd.edu (D.A. Birch), wryoung@ucsd.edu (W.R. Young), pfranks@ucsd.edu (P.J.S. Franks).

0967-0637/$ - see front matter © 2007 Elsevier Ltd. All rights reserved.
doi:10.1016/j.dsr.2007.11.009

individual plankters forming a thin layer have been imaged by Franks and Jaffe (2008) (Fig. 1).

Because thin layers have usually been identified using vertically profiling instruments, their horizontal extent is not well known. Derenbach et al. (1979) suggested a horizontal scale of ~10 m for the layers they observed using a profiling fluorometer coupled with diver observations. Franks (1995) hypothesized that along-isopycnal patch scales of <1 km would generate thin layers through shearing by near-inertial waves. Dekshenieks et al. (2001) and McManus et al. (2003) showed that thin layers of phytoplankton fluorescence had horizontal scales of 5 km or less in a long, narrow fjord.

Recently Franks and Jaffe (2008) used an imaging fluorometer system and found thin layers of cell *types* (defined by their shape and size) that did not appear as layers of enhanced biomass or fluorescence. Thin layers of zooplankton have also been observed using visual (Jaffe et al., 1998) and acoustic techniques (Holliday et al., 2003; McManus et al., 2005). Alldredge et al. (2002) observed a thin layer of marine snow in a vertical profile of closely spaced photographs.

Thin layers are a significant source of small-scale vertical heterogeneity in the marine environment. Herbivorous zooplankton are known to have behaviors that enable them to exploit patches of phytoplankton by turning more frequently in regions of higher phytoplankton concentration and swimming straighter in regions of lower phytoplankton concentration—this results in the zooplankton spending more time where there is more phytoplankton to graze on (e.g., Tiselius, 1992). Thus thin layers of high biomass may be sites of significantly enhanced trophic coupling. High-biomass layers will have smaller nearest-neighbor distances, with potentially greater competition, nutrient recycling, infection, grazing, and sexual exchange than the surrounding waters. Dense concentrations of certain species, for example, a toxic alga (Rines et al., 2002) may actually provide a refuge from grazing pressures. Understanding the dynamics that lead to thin-layer formation will

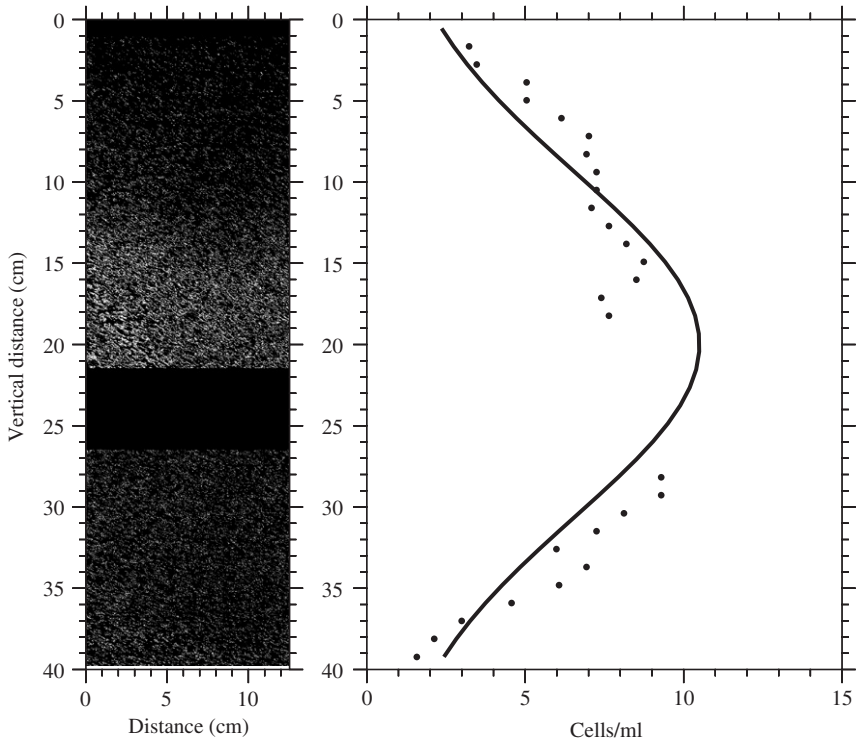

Fig. 1. An example of a thin layer imaged *in situ* with a planar laser imaging fluorometer (Franks and Jaffe, 2008). The left panels show a sequence of images spanning a 40 cm vertical distance. The images show the chlorophyll *a* fluorescence of individual plankters. There is a gap between the images from 21.5 to 26 cm. The right panel shows fluorescent particle counts in 1 cm vertical bins. The solid line is a Gaussian fit to the particle counts.

increase our understanding of the dynamics structuring marine ecosystems and the biogeochemical fluxes they mediate.

Despite their apparent ubiquity, the dynamics of thin layers are not well understood. Both physical and biological mechanisms for the formation of thin layers have been proposed; the actual dynamics are probably a combination of physical and biological factors whose importance varies with time and space. Examples of biological processes that may influence the formation of thin layers include swimming, growth, the inhibition of grazing, and the increase in local viscosity by exudates. Swimming is definitely important to some kinds of thin layers, such as those formed by dinoflagellates and zooplankton (e.g., Rasmussen and Richardson, 1989; McManus et al., 2005). Reproduction may be important to some kinds of thin layers, especially those formed during blooms (Nielsen et al., 1990). Zooplankton may avoid certain kinds of phytoplankton layers, and this may help maintain those layers (Fiedler, 1982). Finally, phytoplankton may also increase the local viscosity and therefore decrease the turbulent diffusion of thin layers (Jenkinson and Biddanda, 1995).

While biological dynamics are undoubtedly important in thin-layer formation, it is essential to fully understand the role of physical mechanisms. Physical processes are generally more easily measured in the field, and provide a useful null hypothesis for layer formation. Layer formation by sinking particles decelerating through a pycnocline has been proposed as a mechanism for the formation of phytoplankton (Derenbach et al., 1979) and marine snow (Alldredge et al., 2002) layers. Franks (1995) explored the creation of thin layers of plankton by the vertical shear of near-inertial internal waves. Because of the oscillating nature of these waves, the layers shown by Franks were transient reversible features which disappeared after a full inertial period. Johnston et al. (2008) examined thin layers formed by shear in the transition zone during an upwelling relaxation event.

Here we investigate the simplest physical mechanism which might be responsible for the formation of thin layers: Eckart (1948) noted that vertically-sheared horizontal currents create sharp vertical property gradients from weak horizontal gradients (see also Osborn, 1998). This fact is the basis of our hypothesis that vertically-sheared horizontal currents are important in forming thin layers. Building on the work of Eckart (1948) and Novikov (1958) we explore the effects of steady shear and diffusion on the formation of a thin layer from an initial patch of plankton. Several of the results contained in this paper are also found in Young et al. (1982), Rhines and Young (1983) and Stacey et al. (2007). We obtain these results in the context of an explicit model for the formation of thin layers whereas Rhines and Young (1983) consider mixing of a passive tracer and Stacey et al. (2007) begins with an equation for the evolution of an abstract layer thickness.

Section 2 describes a simple physical model for the formation of thin layers and presents analysis of the layer properties. The mathematical details of this analysis are contained in Appendix A. Section 3 adds nutrients and plankton growth to our physical model and Appendix B contains the details of the analysis of the nutrient–phytoplankton (*NP*) model. Section 4 contains a summary and discussion of our results.

2. The simplest physical model of thin layers

The basis of this work is a kinematic model showing that a steady vertical shear thins an initial patch of plankton with large vertical scale into a layer that is thin in the vertical (Fig. 2). The model includes diffusion, which tends to counteract the shear-driven layer thinning by dispersing the plankton. Diffusion also decreases the maximum plankton concentration in the patch. Initially we will treat the plankton as an inert passive tracer and ignore all biological processes. The differential equation describing this model is

$$P_t + \alpha z P_x = \kappa_h P_{xx} + \kappa_v P_{zz}. \quad (1)$$

$P(x, z, t)$ is the concentration of plankton at the horizontal position x, vertical position z, and time t. Subscripts of P denote differentiation with respect to the subscripted variable. The parameters are the vertical shear α, the horizontal diffusivity of plankton κ_h, and the vertical diffusivity of plankton κ_v. The variables and their units are summarized in Table 1.

We take as an initial condition a pre-existing patch of plankton with finite horizontal and vertical scales and a concentration that is highest at the center and tapers off toward the edges of the patch. This condition can be modeled as a Gaussian

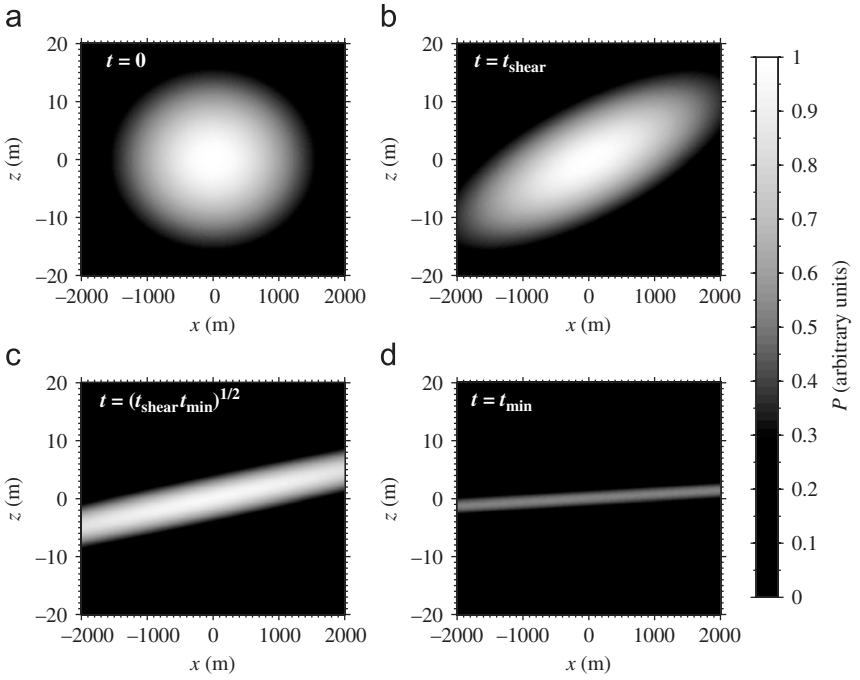

Fig. 2. Solutions of the model in Eq. (1) with the initial condition in Eq. (2). (a) The initial distribution of plankton. (b) The distribution at the end of the tilting phase ($t_{\text{shear}} = 10^4$ s). (c) The distribution of plankton midway through the shear-thinning phase (specifically, at the geometric mean of t_{shear} and t_{min}: $t = \sqrt{t_{\text{shear}} t_{\text{min}}} \approx 11$ h). (d) The distribution at the time of minimum thickness ($t_{\text{min}} \approx 42$ h). The parameters are $L_0 = 1000$ m, $H_0 = 10$ m, $\kappa_{\text{h}} = 1\,\text{m}^2\,\text{s}^{-1}$, $\kappa_{\text{v}} = 10^{-5}\,\text{m}^2\,\text{s}^{-1}$, and $\alpha = 10^{-2}\,\text{s}^{-1}$. The color scale for P is the same in all panels and the units are arbitrary.

Table 1
The variables and their units for the constant-shear model in Eq. (1) with the Gaussian initial condition in Eq. (2)

$P(x,z,t)$	Concentration of plankton (e.g., mg Chl m^{-3})
x	Horizontal coordinate (m)
z	Vertical coordinate (m)
t	Time (s)
α	Vertical shear of the horizontal velocity (s^{-1})
κ_{h}	Horizontal diffusivity of plankton (m^2 s^{-1})
κ_{v}	Vertical diffusivity of plankton (m^2 s^{-1})
$\mathscr{P}$	Total plankton in the xz-plane (e.g., mg Chl m^{-1})
L_0	Initial horizontal extent of the plankton layer (m)
H_0	Initial vertical thickness of the plankton layer (m)
$H(t)$	Vertical thickness of the plankton layer (m)
$L(t)$	Horizontal extent of the plankton layer (m)
$S(t)$	Slope of the layer (dimensionless)
$I(t)$	Layer intensity (dimensionless)
t_{min}	Time of minimum layer thickness (s)
H_{min}	Minimum layer thickness (m), $H_{\text{min}} = H(t_{\text{min}})$
t_{shear}	Shear time (s)
t_{diff}	Diffusion time (s)

distribution of plankton concentration:

$$P(x,z,0) = \frac{\mathscr{P}}{2\pi L_0 H_0} \exp\left(-\frac{x^2}{2L_0^2} - \frac{z^2}{2H_0^2}\right). \qquad (2)$$

The model in Eqs. (1) and (2) assumes that the plankton concentration is uniform in the second horizontal dimension. The total amount of plankton in the patch in the xz-plane in Eq. (2) is $\mathscr{P}$. The maximum plankton concentration, located at $(x,z) = (0,0)$, is $\mathscr{P}/(2\pi L_0 H_0)$, and the initial vertical and horizontal length scales are H_0 and L_0. The patch could represent a region of enhanced biomass formed by some previous event, or it could be a patch of a certain plankton type or community that is distinct from the surrounding community.

We seek solutions of Eqs. (1) and (2) in order to understand the dependence of the layer thickness, extent, and intensity on time, the initial conditions, and the physical parameters (shear and diffusivity). Our main results concerning the smallest possible vertical scale [e.g., the scaling of the minimum layer thickness in Eq. (21)] do not depend on the particular initial condition in Eq. (2), provided that the initial condition has a finite horizontal scale L_0. However, the Gaussian initial condition, Eq. (2), is convenient because it has an analytic solution (derived in Appendix A and illustrated in Fig. 2). This explicit solution enables us to thoroughly explore all aspects of the advection–diffusion model

in Eq. (1) and quantitatively understand shear-driven layer formation and dissipation.

The exact solution for $P(x,z,t)$ given in Appendix A relies on the observation that the plankton distribution maintains its Gaussian structure for all time. Preservation of Gaussianity is a venerable result due to Novikov (1958), who considered a δ-function initial condition. Other work has mainly focused on horizontal shear dispersion (Taylor, 1953; Okubo, 1968; Wilson and Okubo, 1978; Young et al., 1982; Rhines and Young, 1983; Sundermeyer and Ledwell, 2001). Here, instead, we explore the dynamics of the intensity and vertical thickness of layers; these are the properties that are commonly observed with vertically profiling instruments. Our use of the initial condition in Eq. (2), which is a Gaussian patch rather than a δ-function,[1] introduces two new length scales: H_0 and L_0. Our goal is to explain how thin layers form by showing how a patch with initial thickness H_0 is transformed into a layer with thickness $H(t) \ll H_0$.

2.1. Definition of layer thickness $H(t)$, extent $L(t)$, slope $S(t)$, and intensity $I(t)$

Every vertical profile through our model patch $P(x,z,t)$ turns out to be a Gaussian whose standard width is independent of x. Therefore, we define the layer thickness $H(t)$ to be the standard width of the Gaussian profile observed in any vertical profile. Using this definition of the layer thickness we find that the layer thickness of the initial condition $P(x,z,0)$ in Eq. (2) is H_0. The formal definition of $H(t)$ for profiles of any form is given in Eq. (A.16).

To quantify the horizontal extent of a layer we use the root mean square length $L(t)$ defined in Eq. (A.31), which equals the maximum distance in the horizontal from the center of the patch at which the plankton can be detected at a significant fraction [$\exp(-\frac{1}{2}) \approx 61\%$ in our Gaussian model] of the peak plankton concentration at *any* depth in a vertical profile. $L(t)$ is the traditional measure of horizontal scale employed in the shear-dispersion literature (e.g., Sundermeyer and Ledwell, 2001). The analogous quantity in the vertical, the total depth range occupied by the plankton, is much greater than $H(t)$ (Fig. 3).

A signature characteristic of thin layers created by vertical shear is that the layers are tilted across isopycnals. We define $S(t)$ to be the slope one finds by drawing a straight line through the maxima of P in each vertical profile. $S(t)$ is different from the slope of the major axis of an elliptical contour of constant P; if one examines a set of vertical profiles through a phytoplankton patch, it is easier to estimate $S(t)$ than to locate the major axis of the ellipse.

In addition to the size and shape of the layer, we are also interested in the layer intensity $I(t)$, which we define as the ratio of the maximum concentration of plankton divided by the maximum concentration of plankton in the initial condition, Eq. (2). Because of the symmetry of the initial condition, the maximum concentration at any time is $P(0,0,t)$ and therefore the definition of I is equivalent to

$$I(t) \equiv \frac{P(0,0,t)}{P(0,0,0)}. \tag{3}$$

2.2. Weak diffusion

Our discussion will focus on the weak-diffusion regime which is characteristic of oceanic conditions and most relevant to layer formation. Diffusion is weak in the sense that the time to diffuse through L_0 and H_0 is much longer than the advective time scale. To estimate the advective time scale we argue that the differential horizontal velocity on two streamlines separated by H_0 is αH_0. Therefore the time to shear the initial patch by differential horizontal advection through L_0 is

$$t_{\text{shear}} \equiv \frac{L_0}{\alpha H_0}, \tag{4}$$

called t_{start} by Stacey et al. (2007). Forming the ratio of the vertical diffusion time,

$$t_{\text{diff}} \equiv \frac{H_0^2}{\kappa_v}, \tag{5}$$

to t_{shear}, we see that in order for diffusion to be weak we must have

$$\frac{\alpha H_0^3}{L_0 \kappa_v} \gg 1. \tag{6}$$

Comparing the horizontal diffusion time, L_0^2/κ_h, to t_{shear} leads to a second requirement for weak diffusion, namely

$$\frac{\alpha H_0 L_0}{\kappa_h} \gg 1. \tag{7}$$

The non-dimensional combinations above are the Péclet numbers for our model. The assumption of

[1] The special case of a δ-function initial condition can be recovered as the limit $L_0 \to 0$ and $H_0 \to 0$.

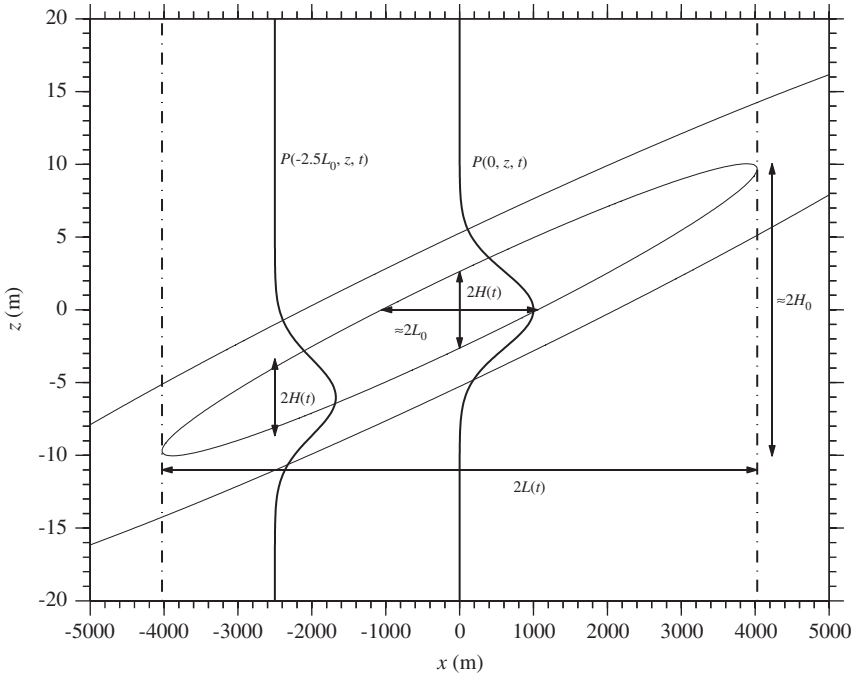

Fig. 3. A schematic of a plankton layer illustrating the definitions of layer thickness $H(t)$ and extent $L(t)$. Note that the layer thickness $H(t)$ is determined by the standard deviation of the Gaussian profiles, not by the distance between any particular contours of constant P. The initial dimensions, L_0 and H_0, are also shown. The total depth range is indicated as $\approx 2H_0$ because in this illustration $t \ll t_{\text{diff}}$, where t_{diff} is the vertical diffusion time scale defined in Eq. (5)—there has not been time for diffusion to transport plankton outside of the initial depth range.

large Péclet number may be justified by considering the results of the coastal mixing and optics (CMO) experiment. One of the major objectives of the CMO experiment was to understand mixing in the vertical over the continental shelf (Dickey and Williams, 2001[2]), which is what dissipates the thin layers in our model. As part of the CMO, MacKinnon and Gregg (2003) found diapycnal diffusivities between 5×10^{-6} and $2 \times 10^{-5}\,\text{m}^2\,\text{s}^{-1}$ over the New England shelf late in the summer of 1996. Ledwell et al. (2004) and Oakey and Greenan (2004) found diapycnal diffusivities between 10^{-6} and $10^{-5}\,\text{m}^2\,\text{s}^{-1}$ in the same place, but not at exactly the same time. During the spring of 1997 MacKinnon and Gregg (2005) found much greater diapycnal diffusivities ($>10^{-3}\,\text{m}^2\,\text{s}^{-1}$), but also sub-critical Richardson numbers, which have been observed to be inconsistent with thin layers (Dekshenieks et al., 2001; McManus et al., 2005). Also as part of the CMO experiment, Sundermeyer and Ledwell (2001) found horizontal diffusivities between 0.3 and $4.9\,\text{m}^2\,\text{s}^{-1}$. Observed shears during the CMO experiment were of order $10^{-2}\,\text{s}^{-1}$ (MacKinnon and Gregg, 2003; Ledwell et al., 2004; Oakey and Greenan, 2004). Given the results of the CMO experiment, we choose $\kappa_h = 1\,\text{m}^2\,\text{s}^{-1}$, $\kappa_v = 10^{-5}\,\text{m}^2\,\text{s}^{-1}$, and $\alpha = 10^{-2}\,\text{s}^{-1}$ as typical values. Using our chosen values for κ_h, κ_v, and α the conditions in (6) and (7) are satisfied for oceanic parameter values if $H_0 \gtrsim 10\,\text{m}$ and $L_0 \gtrsim 100\,\text{m}$.

2.3. The four evolutionary phases

In the case of large Péclet number, the evolution of the plankton distribution obtained from Eqs. (1) and (2) consists of four phases (Fig. 2 shows the first two):

(1) The *tilting phase* during which the initial distribution is tilted and stretched with little change in $H(t)$ or $I(t)$.
(2) The *shear-thinning phase* during which $H(t)$ decreases monotonically, with $H(t) \propto t^{-1}$, until a minimum layer thickness $H_{\min}$ is reached at $t = t_{\min}$.

[2]Volume 106 (2001) of the Journal of Geophysical Research: Oceans is a special issue dedicated to the CMO experiment.

(3) The *decay phase* during which $H(t)$ increases slowly due to vertical diffusion and $I(t)$ decreases to very low levels.
(4) The *shear-dispersion phase*, beginning at $t = t_{\text{diff}}$, when $H(t)$ has finally grown back to the initial thickness H_0.

Diffusion is negligible during the tilting phase and throughout most of the shear-thinning phase. The end of the shear-thinning phase is reached when the layer is so thin that the weak vertical diffusion is finally able to compete with differential advection. During the decay phase $I(t)$ decreases as $t^{-3/2}$ as the layer erodes via horizontal processes. During the final shear-dispersion phase the intensity is very small, and decreases as t^{-2}. We now discuss these four phases in some quantitative detail.

2.4. The tilting and shear-thinning phases

The assumption that diffusion is very weak allows the evolution of Eq. (1) during the tilting and shear-thinning phases to be approximated by neglecting diffusion

$$P_t + \alpha z P_x = 0. \tag{8}$$

The simplified model in Eq. (8) may be solved by the method of characteristics, giving the solution

$$P(x, z, t) = P(x - \alpha z t, z, 0). \tag{9}$$

With the Gaussian initial condition in Eq. (2), the advective solution in Eq. (9) can be put into the form

$$P(x, z, t) = \frac{\mathscr{P}}{2\pi L_0 H_0} \exp\left(-\frac{x^2}{2L^2(t)} - \frac{[z - S(t)x]^2}{2H^2(t)} \right), \tag{10}$$

where

$$H(t) \equiv \frac{L_0 H_0}{\sqrt{L_0^2 + H_0^2 \alpha^2 t^2}}, \tag{11}$$

$$L(t) \equiv \sqrt{L_0^2 + H_0^2 \alpha^2 t^2}, \tag{12}$$

$$S(t) \equiv \frac{H_0^2 \alpha t}{L_0^2 + H_0^2 \alpha^2 t^2}. \tag{13}$$

The non-diffusive equation for $L(t)$ in Eq. (12) is a very good approximation to the full solution through the decay phase (the difference is indistinguishable in Fig. 4). Eqs. (11) and (13) are good approximations for the layer thickness and slope through the shear-thinning phase.

The expression in Eq. (10) shows that for every x the vertical profile of $P(x, z, t)$ has a Gaussian form with thickness $H(t)$, centered about the depth $z = S(t)x$. In other words, the developing layer is tilted along the line

$$z = S(t)x. \tag{14}$$

The slope $S(t)$ in Eq. (13) increases from zero and achieves a maximum $S_{\max} = H_0/(2L_0)$ at time t_{shear} defined in Eq. (4). We define the tilting phase to be when

$$0 \leqslant t \leqslant t_{\text{shear}}. \tag{15}$$

During the tilting phase the patch is distorted by differential advection with little change in $H(t)$. At the end of the tilting phase, when $t = t_{\text{shear}}$, the layer thickness $H(t)$ is approximately[3] $H_0/\sqrt{2} \approx 0.7 H_0$. The maximum concentration of plankton in the layer at the end of the tilting phase is still indistinguishable from the initial maximum concentration (see Appendix A.2 for details). The duration of the tilting phase is determined by the initial patch size and the strength of the shear; for shears less than $10^{-2}\,\text{s}^{-1}$, an initial patch $L_0 = 1\,\text{km}$ wide by $H_0 = 10\,\text{m}$ thick tilts, with little thinning, for 3 h or more.

The shear-thinning phase begins when $t = t_{\text{shear}}$, and continues until the minimum layer thickness $H_{\min}$ is achieved at $t = t_{\min}$. Thus the shear-thinning phase occurs when

$$t_{\text{shear}} \leqslant t \leqslant t_{\min}. \tag{16}$$

The time $t_{\min}$ is estimated below in Eq. (22), and if diffusion is weak then $t_{\min} \gg t_{\text{shear}}$, so that the shear-thinning phase lasts much longer than the tilting phase.

During the beginning of the shear-thinning phase the layer thickness in (11) can be approximated by

$$H(t) \approx \frac{L_0}{\alpha t}, \tag{17}$$

(Fig. 5) and the slope in Eq. (13) becomes

$$S(t) \approx \frac{1}{\alpha t}. \tag{18}$$

We emphasize that the slope of the layer is independent of the initial parameters L_0 and H_0, and that the layer thickness $H(t)$ is independent of the initial layer thickness H_0. Instead, the initial

[3]This estimate follows from inserting (4) into (11).

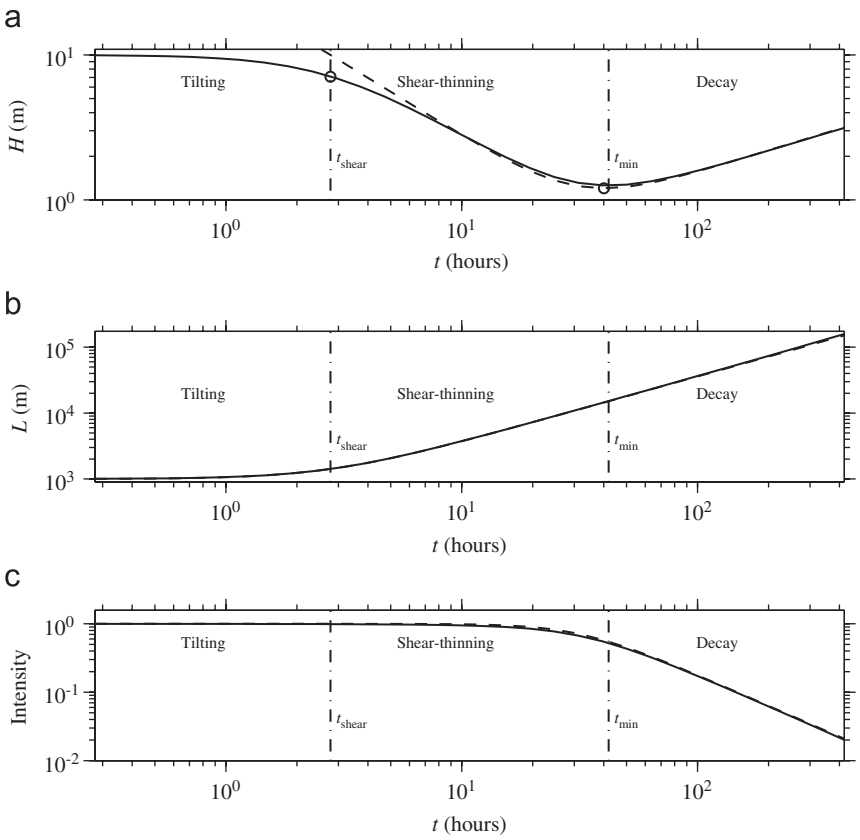

Fig. 4. The layer thickness, extent, and intensity as a function of time. The final time on all three plots is $10t_{min}$ and the parameters are $L_0 = 1000\,\mathrm{m}$, $H_0 = 10\,\mathrm{m}$, $\kappa_h = 1\,\mathrm{m^2\,s^{-1}}$, $\kappa_v = 10^{-5}\,\mathrm{m^2\,s^{-1}}$, and $\alpha = 10^{-2}\,\mathrm{s^{-1}}$. The vertical dashed lines are located at t_{shear}, the end of the tilting phase defined in Eq. (4), and t_{min}, the end of the shear-thinning phase. The shear-dispersion phase occurs for $t \gg 10t_{min}$ and may be seen in Fig. 6. (a) The layer thickness as a function of time. The ○'s are the approximations for layer thickness at the end of the tilting phase in Eq. (11) and at the approximate time of minimum layer thickness in Eq. (A.28). The dashed line is the approximation to $H(t)$ in Eq. (26). (b) The layer extent as a function of time; the dashed line is the approximation to $L(t)$ in Eq. (12) and is indistinguishable from the solid line. (c) The layer intensity as a function of time. The dashed line is the approximation to the intensity in Eq. (23) using the approximation for t_{min} in Eq. (A.26).

layer *width* L_0 determines the thickness of the layer in Eq. (17).

Both the layer thickness and slope decrease with time as $(\alpha t)^{-1}$ during the shear-thinning phase. The approximation in Eq. (17) works because the layer thickness is determined by the vertical separation between the upstream and downstream edges of the patch of plankton-rich water. The difference between the distances travelled by two plankters, one on each edge of the patch and having the same x coordinate, is $2H\alpha t$, where $2H\alpha$ is the difference of the velocities of the two plankters and t is the elapsed time. This difference in distance travelled must equal the distance a particle from the upstream edge has to travel to catch up with a particle from the downstream edge, which is approximately $2L_0$ (Fig. 5). The relationship in Eq. (17) is only approximately true because with the initial condition in Eq. (2), the upstream and downstream edges of the patch are not perfectly parallel and Eq. (17) does not include diffusion. Stacey et al. (2007) contains an alternative explanation of this t^{-1} thinning based on the angle of the layer with the horizontal.

2.5. Minimum layer thickness

If $\kappa_v > 0$, then the shear thinning of the layer cannot continue indefinitely; eventually the layer becomes so thin, and the vertical gradient of P so large, that diffusion halts the thinning regime in Eq. (17). This signifies the end of the shear-thinning phase and occurs at $t = t_{min}$. Here we use simple scaling arguments to estimate t_{min}, H_{min}, and the intensity $I(t_{min})$.

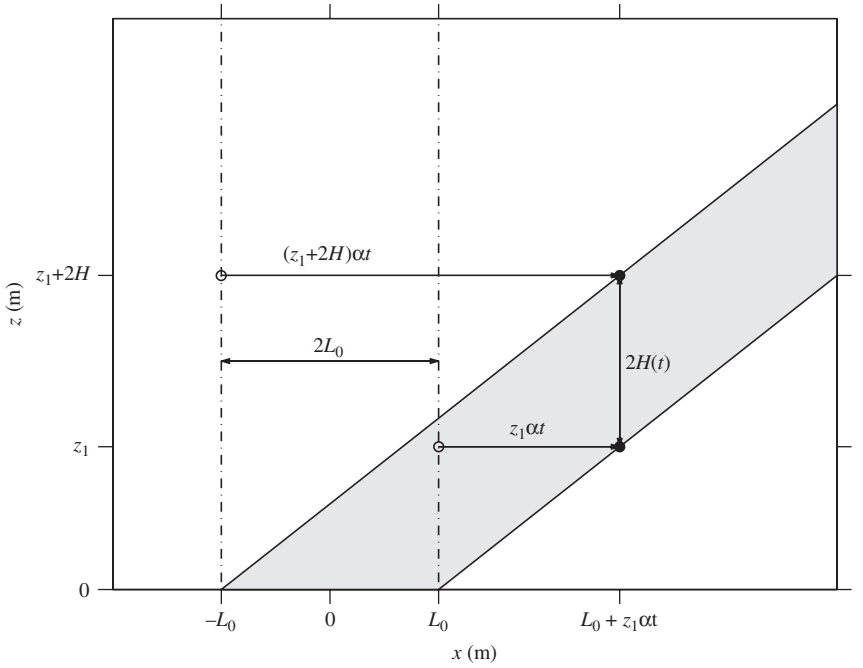

Fig. 5. A schematic of the shear thinning of the advection-only model in Eq. (8) with the initial condition in Eq. (2). As time increases the initial patch rotates and stretches. The distance in the vertical between the two points indicated by the •'s is $2H(t)$. The initial locations of the points are indicated by the ○'s. The difference of the distances travelled by the two points is $2H\alpha t$, which is also $2L_0$—this can be seen in the figure where $L_0 + z_1\alpha t = -L_0 + (z_1 + 2H)\alpha t$.

The minimum layer thickness occurs when shear thinning (represented by $\alpha z P_x$) is balanced by vertical diffusion (represented by $\kappa_v P_{zz}$):

$$\alpha z P_x \approx \kappa_v P_{zz}. \tag{19}$$

The absolute fluid velocities are unimportant here—only the difference in velocity across the layer matters—therefore the appropriate vertical scale in Eq. (19) is $H_{\min}$, the minimum layer thickness. Until diffusion becomes important the horizontal profiles of plankton concentration are translated in the x-direction without modification and so the horizontal scale remains L_0 (Fig. 5). Therefore, using the scale estimates $\partial_z \sim H_{\min}^{-1}$ and $\partial_x \sim L_0^{-1}$, Eq. (19) leads to the scaling

$$\frac{\alpha H_{\min}}{L_0} \sim \frac{\kappa_v}{H_{\min}^2}, \tag{20}$$

which may be rearranged to give the scaling of the minimum layer thickness:

$$H_{\min} \sim \alpha^{-1/3} \kappa_v^{1/3} L_0^{1/3}. \tag{21}$$

The minimum layer thickness in Eq. (21) depends only on the shear α, the vertical diffusivity κ_v, and the initial horizontal width of the patch L_0; the initial patch thickness H_0 is irrelevant to $H_{\min}$. Stacey et al. (2007) contains an alternative derivation of Eq. (20) based on the slope of the layer. For a patch with initial horizontal extent 1 km, a vertical shear of $10^{-2}\,s^{-1}$, and a vertical diffusivity of $10^{-5}\,m^2\,s^{-1}$, the thinnest layers would be about 1 m thick. This is the same thickness as many of the thin layers that have been observed in coastal waters around the world (Dekshenieks et al., 2001; Johnston et al., 2008).

We estimate $t_{\min}$ by combining Eq. (21) with the approximate expression for $H(t)$ in Eq. (17):

$$t_{\min} \sim \alpha^{-2/3} \kappa_v^{-1/3} L_0^{2/3}. \tag{22}$$

Young et al. (1982), Rhines and Young (1983) and Stacey et al. (2007) also derive Eq. (22).

The approximation for $t_{\min}$ in Eq. (22) shows that the time required to achieve the minimum layer thickness $H_{\min}$ has no dependence on the initial layer thickness H_0. With the same shear and diffusivities as above, a patch initially 1 km wide would reach its minimum in about 1 day.

More precise estimates of $H_{\min}$ and $t_{\min}$ in Eqs. (A.28) and (A.26) show that the scale estimates in Eqs. (21) and (22) are correct to within a factor of $3^{1/6} \approx 1.2$ and $3^{1/3} \approx 1.4$, respectively.

The layer intensity $I(t)$ changes only slightly during the tilting and shear-thinning phases. Specifically, $I(t)$ is given by Eq. (A.36), which in dimensional variables is

$$I(t) \approx \frac{1}{\sqrt{1+2(t/t_{\min})^3}}. \tag{23}$$

When $t \ll t_{\min}$ the intensity is approximately 1 (see Fig. 4). At the time of minimum thickness the intensity is

$$I(t_{\min}) \approx \frac{1}{\sqrt{3}}. \tag{24}$$

Since $3^{-1/2} \approx 0.58$, we see that despite thinning by a factor of order 10 between $t = 0$ and $t = t_{\min}$ (as in Fig. 4), the intensity decreases by less than a factor of 2. Because only diffusion can change the concentration of plankton in a water parcel in our advection–diffusion model in Eq. (1), this modest reduction in intensity is consistent with diffusion not being important until $t \gtrsim t_{\min}$.

These scalings suggest that an initial patch of plankton will form layers about 1 m thick over a time scale of days, with very little decrease in concentration during the shear thinning. The minimum layer thickness depends on the initial horizontal scale of the patch, the shear, and the vertical diffusivity. The initial vertical scale and the horizontal diffusivity are irrelevant.

2.6. The decay phase

The decay phase occurs while

$$t_{\min} \leqslant t \leqslant t_{\text{diff}}, \tag{25}$$

where t_{diff} is defined in Eq. (5). During this phase the layer thickness slowly grows and the layer intensity decays. During the decay phase the approximation in Eq. (23) continues to describe the reduction of $I(t)$. The exact solution for $H(t)$ in Eq. (A.18) may be simplified to give an approximate expression for the layer thickness:

$$H(t) \approx H_{\min}\sqrt{\frac{2}{3}\frac{t}{t_{\min}} + \frac{1}{3}\left(\frac{t_{\min}}{t}\right)^2}. \tag{26}$$

The result above applies during both the shear-thinning phase[4] and the decay phase, and fails only at short times when $t < t_{\text{shear}}$ and at extremely long times when $t \gtrsim t_{\text{diff}} \gg t_{\min}$ (Fig. 6).

[4]When $t \ll t_{\min}$ the approximation in Eq. (26) reduces to our earlier expression for $H(t)$ in Eq. (17).

2.7. The lifespan of a thin layer

The importance of a thin layer to the dynamics of the planktonic ecosystem will depend on its duration. A layer that is transient relative to growth and grazing rates will have less effect on the ecosystem dynamics than one that persists for multiple generations. Most phytoplankton have generation times of about a day, and there is a dominant diel periodicity to most trophic interactions; thin layers that persist for days to weeks are likely to be a significant local perturbation to the plankton dynamics. To obtain a simple definition of the lifetime of a thin layer we say that the layer is "thin" while

$$H_{\min} \leqslant H(t) \leqslant 2H_{\min}. \tag{27}$$

From (26) we find that the inequality above is satisfied when

$$0.3t_{\min} \leqslant t \leqslant 6t_{\min}. \tag{28}$$

Thus, according to the definition in Eq. (27), the layer lifespan is approximately $5.7t_{\min}$. However, toward the end of the period in Eq. (28), the layer has suffered significant erosion: substituting $t = 6t_{\min}$ into Eq. (23) we find $I(6t_{\min}) \approx 0.05$, or 5% of the initial maximum. The point is that $I(t)$ is much greater during the shear-thinning phase than during the decay phase. This asymmetry is a consequence of the much greater horizontal extent of the layer during the shear-dispersion phase. Thus Eq. (27) is not a completely satisfactory definition of the lifetime of a layer.

An alternative measure of layer lifetime is the time from when the layer thins to twice the minimum thickness until the layer intensity decays to half the intensity at the time of minimum thickness. With this alternative definition, the thin-layer lifetime is

$$0.3t_{\min} \leqslant t \leqslant 1.8t_{\min}, \tag{29}$$

so that the lifespan is $1.5t_{\min}$.

The main point here is that different definitions of layer lifetime all lead to the same result: thin, intense layers have lifespans of the same order as the time to achieve minimum layer thickness, $t_{\min}$. Under typical oceanic conditions, we expect thin layers to last several days to a week or so.

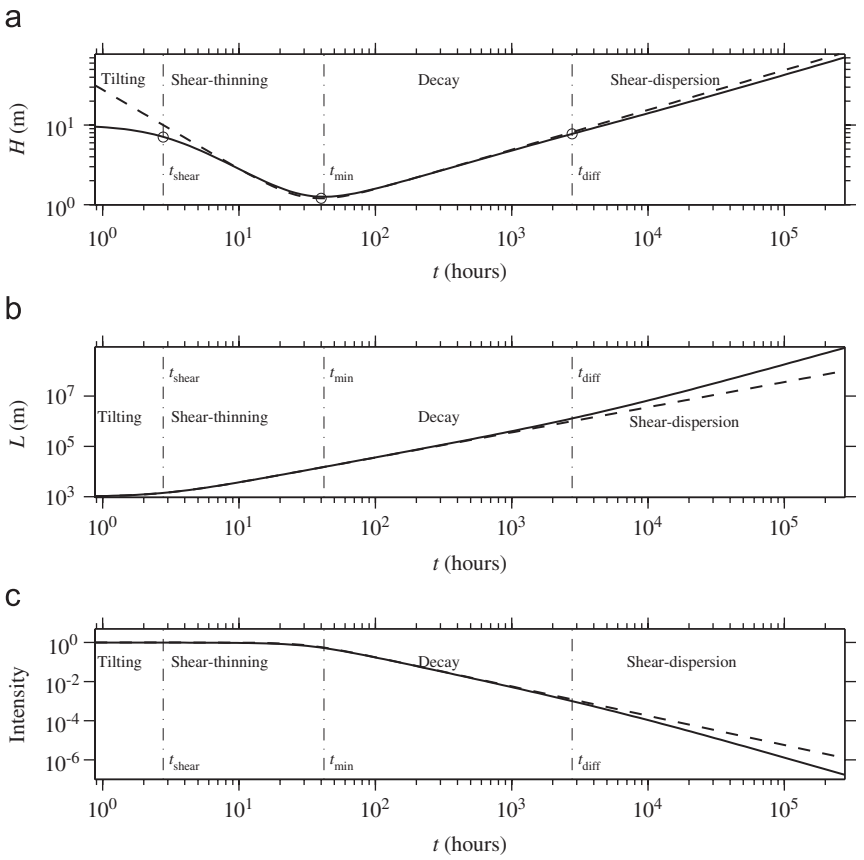

Fig. 6. The layer thickness, extent, and intensity as a function of time, with the final time extended to show the shear-dispersion phase. The final time on all three plots is 10^9 s (about 30 years) and the parameters are $L_0 = 1000\,\mathrm{m}$, $H_0 = 10\,\mathrm{m}$, $\kappa_h = 1\,\mathrm{m^2\,s^{-1}}$, $\kappa_v = 10^{-5}\,\mathrm{m^2\,s^{-1}}$, and $\alpha = 10^{-2}\,\mathrm{s^{-1}}$. The vertical dashed lines are located at t_{shear}, the end of the tilting phase defined in Eq. (4); t_{min}, the end of the shear-thinning phase; and t_{diff}, the end of the shear-dispersion phase. (a) The layer thickness as a function of time. The ○'s are the approximations for layer thickness at the end of the tilting phase, at the approximate time of minimum layer thickness, and at the beginning of the shear-dispersion phase. The dashed curve is the approximation in Eq. (26). (b) The horizontal layer extent as a function of time. The dashed curve is the approximation in Eq. (12). (c) The layer intensity as a function of time—the change in slope from $t^{-3/2}$ to t^{-2} may be seen at $t = t_{diff}$. The dashed curve is the approximation to the intensity in Eq. (23) using the approximation for t_{min} in Eq. (A.26).

2.8. The shear-dispersion phase

For the sake of completeness, we discuss the shear-dispersion phase, during which shear dispersion destroys what little remains of the layer. We define the shear-dispersion phase to be when

$$t_{diff} \leqslant t, \tag{30}$$

where the vertical diffusion time, t_{diff}, is defined in Eq. (5). At this time

$$H(t_{diff}) \approx \sqrt{\tfrac{3}{5}} H_0, \tag{31}$$

and thus a main characteristic of shear dispersion is that the layer thickness finally approaches and then exceeds its initial value H_0. A second important characterization of the shear-dispersion phase is that Eq. (12) finally fails and instead the horizontal extent of the faint remnant grows like $L(t) \sim t^{3/2}$. The shear-dispersion phase is not of much relevance to the study of thin layers because

$$I(t_{diff}) \approx \frac{\kappa_v L_0}{\alpha H_0^3} \ll 1. \tag{32}$$

Thus one might just as well refer to the shear-dispersion phase as the oblivion phase. The approximation for $I(t)$ in Eq. (23) fails at these very long times $t > t_{diff}$; the intensity in the shear-dispersion phase decreases faster than in the decay phase, decreasing like t^{-2} instead of $t^{-3/2}$ [Fig. 6(c)].

One point of interest is that during the shear-dispersion phase $H^2(t) \sim \kappa_v t/2$, so that the "apparent vertical diffusivity" is $\kappa_v/4$.

2.9. The horizontal extent of the layer

Unlike the layer thickness, the layer extent $L(t)$ increases monotonically during all four phases. Eq. (12) applies during the first three phases and begins to fail only when $t \sim t_{\text{diff}}$ and the shear-dispersion phase begins. By evaluating the full equation for layer extent, Eq. (A.31), and keeping only the dominant terms, we find that the horizontal extent of the layer increases by approximately $\sqrt{2}$ during the tilting phase,

$$L(t_{\text{shear}}) \approx \sqrt{2} L_0. \tag{33}$$

At the end of the shear-thinning phase the layer extent has increased to

$$L(t_{\text{min}}) \approx H_0 \left(\frac{3\alpha L_0^2}{\kappa_v} \right)^{1/3}. \tag{34}$$

This is interesting because we see that the initial vertical thickness affects the horizontal extent of the layer. This is because the greater the distance between the top and bottom of the layer, the greater the difference in velocities experienced by the edges of layer and the farther they will separate.

During the final shear-dispersion phase, when $t_{\text{diff}} \ll t$, Eq. (12) is replaced by

$$L(t) \approx \sqrt{\tfrac{2}{3}} \alpha \kappa_v^{1/2} t^{3/2}. \tag{35}$$

The $t^{3/2}$ growth of L is characteristic of shear dispersion in an unbounded region (e.g., Rhines and Young, 1983).

3. Plankton growth

Plankton are of course not inert tracers, and so we consider here a model of an initial patch of nutrients (perhaps due to upwelling or a breaking internal wave injecting nutrients into the euphotic zone) and show how the similarity of plankton growth time scales and the time to minimum layer

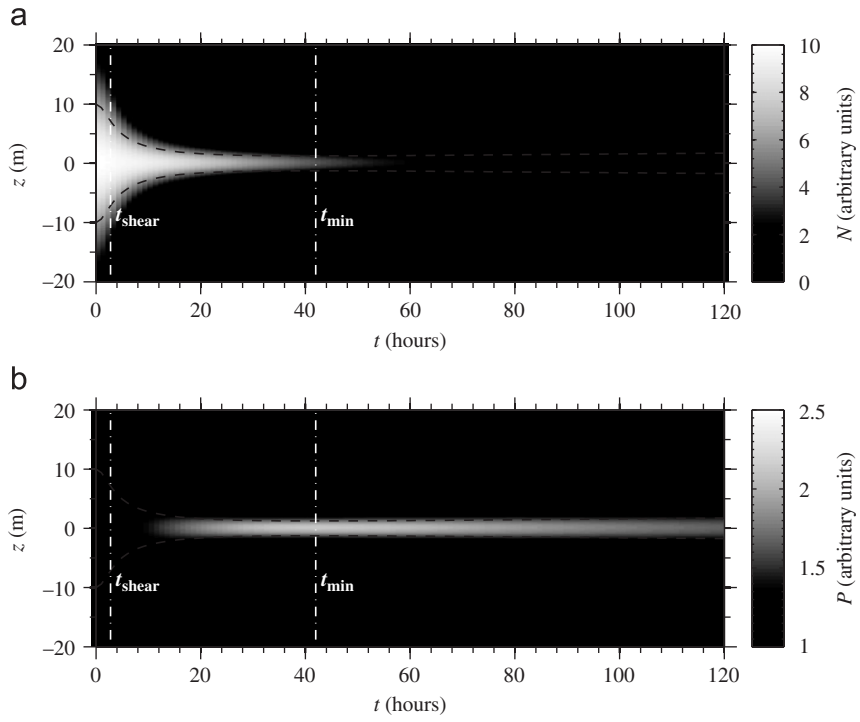

Fig. 7. Vertical profiles of N and P from the system in Eqs. (36) and (37) at $x = 0$ m as a function of time. The parameters are $L_0 = 1000$ m, $H_0 = 10$ m, $\kappa_h = 1\,\text{m}^2\,\text{s}^{-1}$, $\kappa_v = 10^{-5}\,\text{m}^2\,\text{s}^{-1}$, $\alpha = 10^{-2}\,\text{s}^{-1}$, $r = 10^{-5}\,\text{s}^{-1}$, and $N_* = 2\pi L_0 H_0 \mathcal{N} = 10$ (arbitrary units). The dashed black curves are $\pm H(t)$. (a) $N(0, z, t)$. The reduction in vertical scale due to shear thinning is readily apparent for $t < t_{\text{min}}$ and then the nutrients are consumed. (b) $P(0, z, t)$. The plankton is thinning for $t \ll t_{\text{min}}$, but it is hard to see because the plankton intensity is low and then around $t = t_{\text{min}}/2$ an intense thin layer appears.

thickness may cause a thin layer of plankton to appear as if out of nowhere (Fig. 7). The system we consider is the NP model

$$P_t + \alpha z P_x = \frac{rNP}{N_*} + \kappa_h P_{xx} + \kappa_v P_{zz}, \tag{36}$$

$$N_t + \alpha z N_x = -\frac{rNP}{N_*} + \kappa_h N_{xx} + \kappa_v N_{zz}, \tag{37}$$

where the phytoplankton P has a net growth rate rN/N_* when the available nutrient concentration is N. Typical values of rN/N_* in a patch of nutrients are around $10^{-5}\,s^{-1}$; somewhat coincidently, the time for the plankton to use up the patch of nutrients and grow into an intense feature is similar to t_{min}, the time to reach the minimum layer thickness. The dimensions of r are s^{-1} and the dimensions of N and N_* are arbitrary so long as one unit of N can be converted by plankton growth into one unit of P.

For an initial condition we let the concentration of phytoplankton equal a small background level P_0 and take a Gaussian patch with total nutrients $\mathcal{N}$ as the initial nutrient profile

$$P(x,z,0) = P_0, \tag{38}$$

$$N(x,z,0) = \frac{\mathcal{N}}{2\pi L_0 H_0}\exp\left(-\frac{x^2}{2L_0^2} - \frac{z^2}{2H_0^2}\right). \tag{39}$$

We connect to the preceding sections by observing that the quantity $N + P - P_0$ will behave exactly like the plankton patch in Eq. (1) with the initial condition in Eq. (2) and experience all four phases of layer evolution. When we refer to the layer thickness, we really mean the thickness of the anomaly, $P - P_0$, and the linearity of Eq. (1) allowed us to ignore the background plankton concentration P_0. In a model with growth, such as Eqs. (36) and (37), the background concentration is important since phytoplankton must be present to take advantage of a patch of nutrients.

In Appendix B we show that the vertical thickness of the plankton anomaly in the system Eqs. (36) and (37) is the same as the vertical thickness of the layer in the original model in Eq. (1). At times less than t_{min} the plankton distribution in the NP model is thinning as the phytoplankton grow, but the intensity is still low. When measured in the field, this layer might not be considered an interesting feature until t approaches t_{min} and the phytoplankton layer becomes more intense. At times much greater than t_{min} the plankton will have used up all the nutrients and the plankton anomaly, $P - P_0$, in the NP model evolves exactly like P in Eq. (1). The lack of an obvious phytoplankton signal (above the background) during the tilting phase and early part of the shear-thinning phase causes the phytoplankton layer to appear *de novo* as a thin layer, even though the nutrient patch that caused the layer had a larger initial vertical extent.

4. Summary and discussion

To summarize the range of time scales and thicknesses of thin layers we solve Eq. (A.18) numerically to find the minimum layer thickness H_{min} and the time to minimum layer thickness t_{min} as a function of the initial horizontal extent L_0 and the shear α, holding the other parameters fixed (Fig. 8). We take $\kappa_h = 1\,m^2\,s^{-1}$, $\kappa_v = 10^{-5}\,m^2\,s^{-1}$ because these values of diffusivity are the same

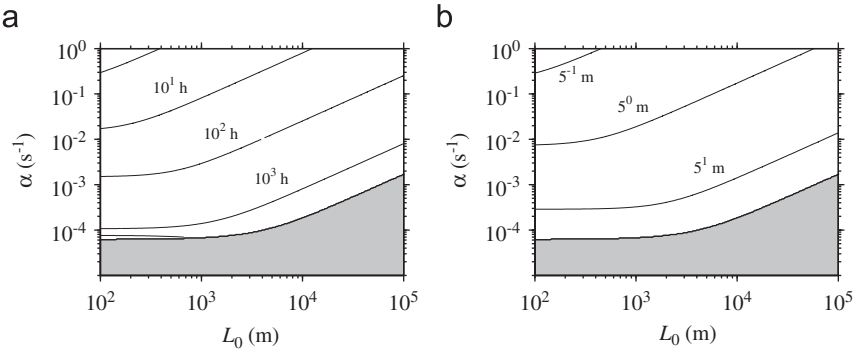

Fig. 8. (a) The time to minimum layer thickness t_{min} as a function of the initial horizontal width L_0 and the shear α. (b) The minimum layer thickness H_{min} as a function of the initial horizontal width L_0 and the shear α. These results are obtained by solving Eq. (A.25) numerically for t_{min} and substituting the results into Eq. (A.18). The parameters in both panels are $\kappa_h = 1\,m^2\,s^{-1}$, $\kappa_v = 10^{-5}\,m^2\,s^{-1}$, and $H_0 = 10\,m$. The shaded regions are where H_0/L_0 is too small and no shear thinning occurs.

order as the horizontal and diapycnal diffusivities found by Sundermeyer and Ledwell (2001), MacKinnon and Gregg (2003), Ledwell et al. (2004), and Oakey and Greenan (2004). From our earlier analyses we have shown that the values of κ_h and H_0 are not relevant in the determination of the layer thickness, so long as H_0 is not so small that the layer does not thin. If $H_0 < 3^{1/6}\alpha^{-1/3}\kappa_v^{1/3}L_0^{1/3}$, then the layer starts as thin as it will ever be and thickens monotonically. Overall, we find that for oceanic parameters, constant shear can produce layers about 1 m thick in a time of order 1 day. Weaker shears produce layers that tilt and thin over periods of weeks before diffusing away. Stronger shears can produce thinner layers with shorter lifetimes in less than 1 day.

The evolution of the steady-shear model in Eq. (1) with Gaussian initial condition in Eq. (2) consists of four phases: the tilting phase, the shear-thinning phase, the decay phase, and the shear-dispersion phase. During the tilting phase the initial patch rotates and stretches in the sheared flow, with little change in its vertical thickness. The tilting phase lasts from $t = 0$ to $t = t_{shear} \equiv L_0/\alpha H_0$, and the layer thickness at t_{shear} is approximately $H_0/\sqrt{2} \approx 0.7H_0$.

After the tilting phase, the layer enters the shear-thinning phase, which lasts until $t = t_{min} \approx 3^{1/3}\alpha^{-2/3}\kappa_v^{-1/3}L_0^{2/3}$. During the shear-thinning phase the layer thickness decreases like t^{-1}, with $H(t) \sim L_0/\alpha t$, until reaching the minimum thickness, $H_{min} \approx 3^{1/6}\alpha^{-1/3}\kappa_v^{1/3}L_0^{1/3}$ at t_{min}. It is at this time that diffusion balances shear thinning and the layer begins to thicken and decay in intensity. Interestingly, the most-studied phase, the shear-dispersion phase, turns out to be irrelevant to thin layers: by the time the shear-dispersion phase begins, the layer intensity has decayed to an insignificant level and the layer thickness is comparable to the initial patch thickness. We also emphasize the importance of initial conditions: just finding the Green's function for Eq. (1) does not reveal the full behavior of the model.

A curious result of our analyses is that the thickness of the layer does not depend on the initial vertical extent of the patch, but rather its horizontal scale. For patches initially 1 km or so wide, vertical shear will create layers ~1 m thick that persist for days to weeks. These time scales are long enough to be biologically relevant: herbivorous zooplankton could find and exploit such layers; the enhanced concentrations could lead to increased sexual exchange or infection within the layers; and particle collisions within high-biomass layers of certain phytoplankton types could lead to aggregation, sinking, and locally episodic carbon fluxes out of the euphotic zone.

The simple *NP* model gives some interesting insights into the time- and space-dependence of phytoplankton layers that might be observed in the field. A nutrient injection to the euphotic zone is sheared as the phytoplankton are growing. This leads not to a thick patch of phytoplankton, but rather the growth of the phytoplankton in an initially thin layer. This is a consequence of the similarities in the time scales for layer tilting and thinning, and phytoplankton growth. By the time the phytoplankton have reached a concentration significantly above the background, the initial patch of nutrients has already undergone significant tilting and thinning. It will be interesting, given the recent availability of technologies such as the *in situ* ultraviolet spectrophotometer (ISUS) optical nitrate sensor (Satlantic, Halifax NS, Canada), to explore these predicted dynamics in the field. Regions such as wind-driven upwelling systems, or flow around topography are likely sites for nutrient injections to the euphotic zone with subsequent phytoplankton growth and shearing.

Our model assumes an initial patch of phytoplankton or nutrients with a finite vertical and horizontal extent. Such a patch could form through, for example, nutrient injection in a coastal wind-driven upwelling system (Johnston et al., 2008), nutrient injection through breaking internal waves, upwelling and patch formation in fronts, meanders, and eddies, or local wind-driven mixing under a storm track. While we have concentrated on the formation of layers of locally enhanced biomass, it is important to recognize that the model applies to any patch of a property. Thus a local patch of a particular community or species of plankton with a biomass indistinguishable from the surrounding community will form a thin layer in a vertically-sheared current. Such layers of properties—even in the absence of any bulk concentration gradients such as chlorophyll concentration—should be ubiquitous features in the ocean.

The simple model in Eq. (1) contains no biological processes; it quantifies for any tracer (e.g. plankton species, plankton community, chemical) Eckart's observation that sheared currents will transform horizontal variability into vertical variability. Given the existence of sheared currents and

horizontal variability (“patchiness”), vertical layers in the ocean are unavoidable.

The layers described here have several diagnostics that should make them detectable in the field. Most importantly, layers formed by vertical shearing of a patch should incline across isopycnals, as most of the vertical shear in the ocean is perpendicular to isopycnal surfaces. Over the horizontal extent $L(t)$ of the layer, the local maximum in intensity will be found on different isopycnals, with one end of the patch in lower-density water, and the opposite end in higher-density water. Vertical shear requires vertical stratification: if the stratification is too weak, the shear will cause turbulent mixing which will erode a layer. Thus we expect thin layers to form in stratified waters, with the thinnest (and shortest-lived) layers forming in the regions of strongest stratification and shear (Fig. 8). Finally, we predict that as technologies are developed, extensive vertical structure of most chemical and biological properties in the ocean will be revealed. Shear is ubiquitous in the ocean, horizontal patchiness is constantly being created, and so thin layers of properties should be expected, rather than surprising.

Acknowledgments

The authors would like to thank Jennifer MacKinnon, Rob Pinkel, and Shaun Johnston for helpful discussions. This work was supported by National Science Foundation Grants OCE-0220362 and OCE-0726320 to W.R.Y., and NSF Grant OCE-0220379 and ONR Grant N00014-06-1-0304 to P.J.S.F.

Appendix A. Gaussian with the method of moments

In this Appendix we present the complete solution to Eq. (1) with initial condition Eq. (2). We also formally define the layer properties, introduce a convenient non-dimensionalization, and derive approximations to the layer properties during the four phases of layer evolution.

First, define the global average of a function f weighted by the distribution $P(x,z,t)$:

$$\langle\!\langle f \rangle\!\rangle \equiv \frac{\int_{-\infty}^{\infty}\int_{-\infty}^{\infty} fP\,\mathrm{d}x\,\mathrm{d}z}{\int_{-\infty}^{\infty}\int_{-\infty}^{\infty} P\,\mathrm{d}x\,\mathrm{d}z}. \tag{A.1}$$

A useful consistency check is to note that $\langle\!\langle 1 \rangle\!\rangle = 1$. Also, note that Eq. (1) conserves the total amount of plankton at all times:

$$\int_{-\infty}^{\infty}\int_{-\infty}^{\infty} P(x,z,t)\,\mathrm{d}x\,\mathrm{d}z = \mathscr{P}. \tag{A.2}$$

We define the second moments[5] of the plankton distribution using the global average defined in Eq. (A.1):

$$m_{11} \equiv \langle\!\langle x^2 \rangle\!\rangle, \quad m_{22} \equiv \langle\!\langle z^2 \rangle\!\rangle, \quad m_{12} \equiv \langle\!\langle xz \rangle\!\rangle. \tag{A.3}$$

We obtain the three second moments of the plankton distribution by applying the same method of moments as Aris (1956) with the initial conditions

$$m_{11}(0) = L_0^2, \quad m_{12}(0) = 0, \quad m_{22}(0) = H_0^2. \tag{A.4}$$

Multiplying Eq. (1) by x^2, xz, and z^2 and averaging according to Eq. (A.1) yields a set of coupled equations for the second moments which may be solved to obtain

$$m_{11}(t) = L_0^2 + 2\kappa_\mathrm{h} t + \alpha^2 H_0^2 t^2 + \tfrac{2}{3}\alpha^2\kappa_\mathrm{v} t^3, \tag{A.5}$$

$$m_{12}(t) = \alpha H_0^2 t + \alpha\kappa_\mathrm{v} t^2, \tag{A.6}$$

$$m_{22}(t) = H_0^2 + 2\kappa_\mathrm{v} t. \tag{A.7}$$

Armed with all of the first and second moments of the plankton distribution we can write down the solution to Eq. (1) with the initial condition in Eq. (2) (van Kampen, 1981)

$$P(x,z,t) = \frac{\mathscr{P}}{2\pi\sqrt{\mathscr{M}(t)}} \exp\left(-\frac{1}{2}\boldsymbol{x}^\mathrm{T} M^{-1}(t)\boldsymbol{x}\right), \tag{A.8}$$

where $\boldsymbol{x}$ is a column vector and M is the moment matrix with determinant $\mathscr{M}$:

$$\boldsymbol{x} \equiv \begin{pmatrix} x \\ z \end{pmatrix}, \quad M(t) \equiv \begin{pmatrix} m_{11}(t) & m_{12}(t) \\ m_{12}(t) & m_{22}(t) \end{pmatrix} \tag{A.9}$$

and

$$\mathscr{M}(t) \equiv \det M(t) = m_{11}m_{22} - m_{12}^2. \tag{A.10}$$

The moment matrix $M(t)$ is real and symmetric and its inverse $M^{-1}(t)$ appearing in Eq. (A.8) is

$$M^{-1}(t) = \frac{1}{\mathscr{M}(t)} \begin{pmatrix} m_{22}(t) & -m_{12}(t) \\ -m_{12}(t) & m_{11}(t) \end{pmatrix}. \tag{A.11}$$

Thus we have now found the complete solution to $P(x,z,t)$. Next we use this solution to examine the layer thickness.

[5]The first moments, $\langle\!\langle x \rangle\!\rangle$ and $\langle\!\langle z \rangle\!\rangle$, are both initially zero and remain zero for all time.

A.1. Layer thickness and extent

To examine properties of the distribution $P(x,z,t)$ in the vertical, such as layer thickness, we must define an average over z only

$$\langle f\rangle \equiv \frac{\int_{-\infty}^{\infty} fP\,\mathrm{d}z}{\int_{-\infty}^{\infty} P\,\mathrm{d}z}. \tag{A.12}$$

To evaluate quantities such as $\langle z\rangle$ we use the expression for $P(x,z,t)$ in Eq. (A.8) and complete the square in the exponential to obtain

$$\langle z^n\rangle = \frac{1}{\sqrt{\pi}}\int_{-\infty}^{\infty}\left(\sqrt{\frac{2\mathscr{M}}{m_{11}}}\zeta + \frac{m_{12}}{m_{11}}x\right)^n \mathrm{e}^{-\zeta^2}\,\mathrm{d}\zeta. \tag{A.13}$$

Specifically, the center of mass of any vertical profile is

$$\langle z\rangle = \frac{m_{12}}{m_{11}}x. \tag{A.14}$$

Similarly,

$$\langle z^2\rangle = \frac{m_{12}^2}{m_{11}^2}x^2 + \frac{\mathscr{M}}{m_{11}}. \tag{A.15}$$

Define the square of the thickness H of any vertical profile to be

$$H^2(x,t) \equiv \langle z^2\rangle - \langle z\rangle^2. \tag{A.16}$$

Use Eqs. (A.14) and (A.15) to find the square of the thickness:

$$H^2(x,t) = \frac{\mathscr{M}}{m_{11}} = m_{22} - \frac{m_{12}^2}{m_{11}}, \tag{A.17}$$

or we can save some algebra by observing that Eq. (A.8) shows that for the Gaussian model, the square of the formal layer thickness is the same as $1/M_{22}^{-1}$. Note that Eq. (A.17) shows that $H(x,t)$ is independent of x for our Gaussian distribution, and so we will neglect the x from now on. To obtain an explicit expression for $H(t)$ in terms of t and the parameters of the model, substitute Eqs. (A.7), (A.6), and (A.5) into Eq. (A.17):

$$H^2(t) = H_0^2 + 2\kappa_\mathrm{v}t - \frac{\alpha^2\kappa_\mathrm{v}^2t^4 + 2\alpha^2H_0^2\kappa_\mathrm{v}t^3 + \alpha^2H_0^4t^2}{\frac{2}{3}\alpha^2\kappa_\mathrm{v}t^3 + \alpha^2H_0^2t^2 + 2\kappa_\mathrm{h}t + L_0^2}. \tag{A.18}$$

Using the solution for $H(t)$ in Eq. (A.18), we can now find the minimum layer thickness and the time to minimum layer thickness. However, before proceeding any farther, it is advantageous to switch to dimensionless variables. Therefore, we define three dimensionless quantities:

$$\epsilon \equiv \left(\frac{\kappa_\mathrm{v}}{\alpha L_0^2}\right)^{1/3}, \quad \eta \equiv \frac{H_0}{L_0}, \quad \chi \equiv \frac{\kappa_\mathrm{h}}{\kappa_\mathrm{v}}. \tag{A.19}$$

Furthermore, we define the non-dimensional time τ and non-dimensional thickness h:

$$\tau \equiv \epsilon\alpha t, \quad h \equiv \frac{H}{\epsilon L_0}. \tag{A.20}$$

Now express the equation for layer thickness, Eq. (A.18), in non-dimensional variables

$$h^2(\tau) = \frac{\epsilon^2\tau^4 + 2\eta^2\tau^3 + 12\epsilon^4\chi\tau^2 + 6\epsilon^2(1+\eta^2\chi)\tau + 3\eta^2}{2\epsilon^2\tau^3 + 3\eta^2\tau^2 + 6\epsilon^4\chi\tau + 3\epsilon^2}. \tag{A.21}$$

We obtain an approximate equation for the layer thickness as a function of time by dropping all of the terms containing ϵ from the right-hand side of Eq. (A.21)

$$h^2(\tau) \approx \frac{2\tau^3+3}{3\tau^2}. \tag{A.22}$$

Implicit in this simplification is the assumption that

$$\chi \ll \epsilon^{-2}, \tag{A.23}$$

which corresponds to ignoring the term κ_h/L_0^2 in the scaling argument in Eq. (20).

Let τ_min be the time of minimum layer thickness. Then

$$\left.\frac{\mathrm{d}[h^2]}{\mathrm{d}\tau}\right|_{\tau=\tau_\mathrm{min}} = 0, \tag{A.24}$$

or equivalently,

$$\tau_\mathrm{min}^4 - 3\tau_\mathrm{min} \approx 0. \tag{A.25}$$

We ignore the root $\tau_\mathrm{min} \approx 0$ and take the only remaining real root, $\tau_\mathrm{min} \approx 3^{1/3}$. Using the definition of τ in Eq. (A.20) we find t_min, the time of minimum layer thickness, in dimensional variables

$$t_\mathrm{min} \approx 3^{1/3}\alpha^{-1}\left(\frac{\alpha L_0^2}{\kappa_\mathrm{v}}\right)^{1/3}. \tag{A.26}$$

To find an approximation for H_min, the minimum layer thickness, substitute $\tau = 3^{1/3}$ into Eq. (A.22),

$$h_\mathrm{min} \approx 3^{1/6}. \tag{A.27}$$

Using Eq. (A.27) and the definition of ϵ in Eq. (A.19) yields an approximation to the minimum

layer thickness in dimensional variables

$$H_{\min} \approx 3^{1/6} L_0 \left(\frac{\kappa_v}{\alpha L_0^2} \right)^{1/3}. \tag{A.28}$$

We would also like to know the time at which the layer has a particular thickness. To find τ as a function of H we rearrange the equation for layer thickness, Eq. (A.22), as a cubic polynomial in time

$$2\tau^3 - 3h^2\tau^2 + 3 = 0. \tag{A.29}$$

If h is large (and $2 \times 3^{1/6}$ is large enough), then the two positive roots of Eq. (A.29) are

$$\tau \approx \frac{1}{h} \quad \text{and} \quad \frac{3h^2}{2}. \tag{A.30}$$

Both roots in Eq. (A.30) are times when the layer thickness is $3^{-1/6} h H_{\min}$; the first is during the shear-thinning phase and the second is during the shear-dispersion phase. Note that when $t \gg t_{\min}$ then the τ^4 term in Eq. (A.21) is important and Eq. (A.29) and its roots Eq. (A.30) are incorrect. Appendix A.3 contains an approximation for $H(t)$ for very large times.

We define the horizontal extent of the layer $L(t)$ to be

$$L(t) \equiv \sqrt{m_{11}}. \tag{A.31}$$

Note that the horizontal analog of $H(t)$ in Eq. (A.17) is $m_{11} - m_{12}^2/m_{22}$, which is the horizontal thickness (as opposed to the horizontal extent) of the layer. However, we choose not to examine $m_{11} - m_{12}^2/m_{22}$ because we focus on quantities observed by vertical (not horizontal) profiles.

A.2. Layer intensity

To obtain an equation for the layer intensity we substitute the solution for P, Eq. (A.8), into the definition of I, Eq. (3):

$$I \equiv \frac{P(0,0,t)}{P(0,0,0)} \tag{A.32}$$

$$= \sqrt{\frac{\mathscr{M}(0)}{\mathscr{M}(t)}} \tag{A.33}$$

$$= \left[1 + \left(\frac{2\kappa_v}{H_0^2} + \frac{2\kappa_h}{L_0^2} \right) t + \frac{4\kappa_v \kappa_h}{H_0^2 L_0^2} t^2 + \frac{2\alpha^2 \kappa_v}{3L_0^2} t^3 + \frac{\alpha^2 \kappa_v^2}{3H_0^2 L_0^2} t^4 \right]^{-1/2}. \tag{A.34}$$

Using the definitions of ϵ, η, and χ and writing t as $\alpha^{-1}\epsilon^{-1}\tau$ one may rewrite Eq. (A.34) as

$$I(\tau) = [1 + 2\epsilon^2(\eta^{-2} + \chi)\tau + 4\epsilon^4 \eta^{-2} \chi \tau^2 + \tfrac{2}{3}\tau^3 + \tfrac{1}{3}\epsilon^2 \eta^{-2} \tau^4]^{-1/2}. \tag{A.35}$$

Neglecting all terms containing ϵ in Eq. (A.35) yields a simple equation for the approximate layer intensity as a function of time (as long as τ is large enough so that the τ^3 term is larger than the τ^1 term, but not so large that the τ^4 is relevant)

$$I(\tau) \approx \frac{1}{\sqrt{1 + \frac{2}{3}\tau^3}}. \tag{A.36}$$

Substituting the value $\tau = 3^{1/3}$ ($t = t_{\min}$) into Eq. (A.36) one obtains the layer intensity at the approximate time of minimum layer thickness:

$$I(t_{\min}) \approx 3^{-1/2}. \tag{A.37}$$

At $t = t_{\text{shear}}$, the end of the tilting phase, $\tau_{\text{shear}} = \epsilon\eta^{-1}$ and Eq. (A.36) says that the layer intensity is indistinguishable from 1.

We can also find time as a function of intensity by inverting Eq. (A.36):

$$\tau \approx \left(\frac{3I^{-2} - 3}{2} \right)^{1/3}. \tag{A.38}$$

Eq. (A.38) has one real root, which is consistent with the layer intensity monotonically decreasing with time.

A.3. Long-time behavior and the shear-dispersion phase

The approximations for layer thickness in Eqs. (A.30) and intensity (A.36) are only good when τ in Eq. (A.20) is not too large; eventually the τ^4 terms in the full equations [Eqs. (A.21) and (A.35)] dominate and new approximations for the layer thickness and intensity become necessary. The τ^4 terms become important when they are of the same order as the τ^3 terms in Eqs. (A.21) and (A.35). This happens when $t \sim t_{\text{diff}}$ or equivalently

$$\tau = \tau_{\text{diff}} \equiv \frac{\eta^2}{\epsilon^2}. \tag{A.39}$$

Substituting Eq. (A.39) into the full equations for thickness, Eq. (A.21), we find

$$h(\tau_{\text{diff}}) \approx \sqrt{\frac{3}{5}} \frac{\eta}{\epsilon}, \tag{A.40}$$

which means that before the τ^4 terms dominate and Eqs. (A.44) and (A.42) apply, the layer is almost as thick as when it started. Similarly, the full equation for layer intensity, Eq. (A.35), shows that

$$I(\tau_{\text{diff}}) \approx \frac{\epsilon^3}{\eta^3} \ll 1 \tag{A.41}$$

and the layer intensity is tiny before Eqs. (A.44) and (A.42) apply.

For the sake of completeness we note the long time behavior of H, L, and I:

$$h^2(\tau) \sim \frac{\tau}{2}, \quad \tau \to \infty, \tag{A.42}$$

$$L(\tau) \sim \sqrt{\tfrac{2}{3}} L_0 \epsilon^{3/2} \tau^{3/2}, \quad \tau \to \infty, \tag{A.43}$$

$$I(\tau) \sim \sqrt{3}\,\frac{\eta}{\epsilon \tau^2}, \quad \tau \to \infty. \tag{A.44}$$

Finally, we note two interesting properties (both may be found in the δ-function solution of Novikov, 1958) of the long-time behavior shear-dispersion phase. First, the layer thickness is proportional to $t^{1/2}$, as one would see with diffusion alone, but because of the shear the effective diffusion coefficient is one-quarter κ_v. Second, in a purely diffusive system the layer intensity would behave as t^{-1}, but in this system the intensity at long times is proportional to t^{-2}.

Appendix B. Plankton growth

In this appendix we derive an approximation for the short-time behavior of the vertical thickness of the plankton anomaly in the *NP* system [Eqs. (36) and (37)]. First we define

$$Q \equiv N + P. \tag{B.1}$$

Q satisfies the exact same equation as P in Eq. (1),

$$Q_t + \alpha z Q_x = \kappa_h Q_{xx} + \kappa_v Q_{zz}, \tag{B.2}$$

with a slightly different initial condition,

$$Q(x,z,0) = P_0 + \frac{\mathcal{N}}{2\pi L_0 H_0} \exp\left(-\frac{x^2}{2L_0^2} - \frac{z^2}{2H_0^2}\right). \tag{B.3}$$

The solution for Q is

$$Q(x,z,t) = P_0 + \frac{\mathcal{N}}{2\pi\sqrt{\mathcal{M}(t)}} \exp\left(-\frac{1}{2}\boldsymbol{x}^{\mathrm{T}} M^{-1}(t)\boldsymbol{x}\right), \tag{B.4}$$

where $\boldsymbol{x}$, $\mathcal{M}$, and M are the same as in Eqs. (A.9) and (A.10). We obtain an approximation for P during the tilting and shear-thinning phases by neglecting diffusion in Eqs. (36) and (B.2), in which case we can write

$$P(x,z,t) = \frac{P_0 Q(x,z,t)}{P_0 + (Q(x,z,t) - P_0)\exp[-rQ(x,z,t)t/N_*]}, \tag{B.5}$$

$$Q(x,z,t) = Q(x - \alpha z t, z, 0). \tag{B.6}$$

We are really interested in the growth of plankton anomaly,

$$\begin{aligned} P'(x,z,t) &\equiv P(x,z,t) - P_0 \\ &= \frac{P_0[Q(x,z,t) - P_0](1 - \exp[-rQ(x,z,t)t/N_*])}{P_0 + [Q(x,z,t) - P_0]\exp[-rQ(x,z,t)t/N_*]}, \end{aligned} \tag{B.7}$$

which for small t (which is also when we can neglect diffusion) may be approximated by

$$P'(x,z,t)/P_0 \approx rt \exp\left(-\frac{x^2}{2L^2(t)} - \frac{[z - S(t)x]^2}{2H^2(t)}\right), \tag{B.8}$$

with $H(t)$, $L(t)$, and $S(t)$ defined in Eqs. (11), (12), and (13). Therefore we have shown that the *NP* model forms layers with the same thickness as the inert tracer model, Eq. (1).

References

Alldredge, A.L., Cowles, T.J., MacIntyre, S., Rines, J.E.B., Donaghay, P.L., Greenlaw, C.F., Holliday, D.V., Dekshenieks, M.M., Sullivan, J.M., Zaneveld, J.R., 2002. Occurrence and mechanisms of formation of a dramatic thin layer of marine snow in a shallow Pacific Fjord. Marine Ecology Progress Series 233, 1–12.

Aris, R., 1956. On the dispersion of a solute in a fluid flowing through a tube. Proceedings of the Royal Society A: Mathematical and Physical Sciences 235 (1200), 67–77.

Dekshenieks, M.M., Donaghay, P.L., Sullivan, J.M., Rines, J.E.B., Osborn, T.R., Twardowski, M.S., 2001. Temporal and spatial occurrence of thin phytoplankton layers in relation to physical processes. Marine Ecology Progress Series 223, 61–71.

Derenbach, J.B., Astheimer, H., Hansen, H.P., Leach, H., 1979. Vertical microscale distribution of phytoplankton in relation to the thermocline. Marine Ecology Progress Series 1, 181–193.

Dickey, T.D., Williams III, A.J., 2001. Interdisciplinary ocean process studies on the New England shelf. Journal of Geophysical Research 106 (C5), 9427–9434.

Eckart, C., 1948. An analysis of the stirring and mixing processes in incompressible fluids. Journal of Marine Research 7, 265–275.

Fiedler, P.C., 1982. Zooplankton avoidance and reduced grazing responses to *Gymnodinium splendens* (dinophyceae). Limnology and Oceanography 27 (5), 961–965.

Franks, P.J.S., 1995. Thin layers of phytoplankton: a model of formation by near-inertial wave shear. Deep-Sea Research Part I 42 (1), 75–91.

Franks, P.J.S., Jaffe, J.S., 2008. Microscale variability in the distributions of large fluorescent particles observed *in situ* with a planar laser imaging fluorometer. Journal of Marine Systems 69, 254–270.

Holliday, D.V., Donaghay, P.L., Greenlaw, C.F., McGehee, D.E., McManus, M.A., Sullivan, J.M., Miksis, J.L., 2003. Advances in defining fine- and micro-scale pattern in marine plankton. Aquatic Living Resources 16, 131–136.

Jaffe, J.F., Franks, P.J.S., Leising, A.W., 1998. Simultaneous imaging of phytoplankton and zooplankton distributions. Oceanography 11 (1), 24–29.

Jenkinson, I.R., Biddanda, B.A., 1995. Bulk-phase viscoelastic properties of seawater: relationship with plankton components. Journal of Plankton Research 17 (12), 2251–2274.

Johnston, T.M.S., Cheriton, O.M., Pennington, J.T., Chavez, F.P., 2008. Thin phytoplankton layer formation at eddies, filaments, and fronts in a coastal upwelling zone. Deep-Sea Research II, accepted.

Ledwell, J.R., Duda, T.F., Sundermeyer, M.A., Seim, H.E., 2004. Mixing in a coastal environment: 1. A view from dye dispersion. Journal of Geophysical Research 109.

MacKinnon, J.A., Gregg, M.C., 2003. Mixing on the late-summer New England shelf—solibores, shear, and stratification. Journal of Physical Oceanography 33, 1476–1492.

MacKinnon, J.A., Gregg, M.C., 2005. Spring mixing: turbulence and internal waves during restratification on the New England shelf. Journal of Physical Oceanography 35, 2425–2443.

McManus, M.A., Alldredge, A.L., Barnard, A.H., Boss, E., Case, J., Cowles, T.J., Donaghay, P.L., Eisner, L., Gifford, D.J., Greenlaw, C.F., Herren, C.M., Holliday, D.V., Johnson, D., MacIntyre, S., McGehee, D.M., Osborn, T.R., Perry, M.J., Pieper, R.E., Rines, J.E.B., Smith, D.C., Sullivan, J.M., Talbot, M.K., Twardowski, M.S., Weidemann, A., Zaneveld, J.R., 2003. Characteristics, distribution and persistence of thin layers over a 48 h period. Marine Ecology Progress Series 261, 1–19.

McManus, M.A., Cheriton, O.M., Drake, P.J., Holliday, D.V., Storlazzi, C.D., Donaghay, P.L., Greenlaw, C.F., 2005. Effects of physical processes on structure and transport of thin zooplankton layers in the coastal ocean. Marine Ecology Progress Series 301, 199–215.

Nielsen, T.G., Kiørboe, T., Bjørnsen, P.K., 1990. Effects of a *Chrysochromulina polylepis* subsurface bloom on the planktonic community. Marine Ecology Progress Series 62, 21–35.

Novikov, E.A., 1958. Concerning a turbulent diffusion in a stream with a transverse gradient of velocity. Prikladnaya Matematika I Mekhanika 22 (3), 412–414.

Oakey, N.S., Greenan, B.J.W., 2004. Mixing in a coastal environment: 2. A view from microstructure measurements. Journal of Geophysical Research 109.

Okubo, A., 1968. Some remarks on the importance of the "shear effect" on horizontal diffusion. Journal of the Oceanographical Society of Japan 24 (2), 60–69.

Osborn, T.R., 1998. Finestructure, microstructure, and thin layers. Oceanography 11 (1), 36–43.

Rasmussen, J., Richardson, K., 1989. Response of *Gonyaulax tamarensis* to the presence of a pycnocline in an artificial water column. Journal of Plankton Research 11 (4), 747–762.

Rhines, P.B., Young, W.R., 1983. How rapidly is a passive scalar mixed within closed streamlines? Journal of Fluid Mechanics 133, 133–145.

Rines, J.E.B., Donaghay, P.L., Dekshenieks, M.M., Sullivan, J.M., Twardowski, M.S., 2002. Thin layers and camouflage: hidden *pseudo-nitzschia* spp. (bacillariophyceae) populations in a fjord in the San Juan Islands, Washington, USA. Marine Ecology Progress Series 225, 123–137.

Stacey, M.T., McManus, M.A., Steinbuck, J.V., 2007. Convergences and divergences and thin layer formation and maintenance. Limnology and Oceanography 52 (4), 1523–1532.

Strickland, J.D.H., 1968. A comparison of profiles of nutrient and chlorophyll concentrations taken from discrete depths and by continuous recording. Limnology and Oceanography 13 (2), 388–391.

Sundermeyer, M.A., Ledwell, J.R., 2001. Lateral dispersion over the continental shelf: analysis of dye release experiments. Journal of Geophysical Research 106 (C5), 9603–9621.

Taylor, G.I., 1953. Dispersion of soluble matter in solvent flowing slowly through a tube. Proceedings of the Royal Society B: Biological Sciences 219, 186–203.

Tiselius, P., 1992. Behavior of *Acartia tonsa* in patchy food environments. Limnology and Oceanography 37, 1640–1651.

van Kampen, N.G., 1981. Stochastic Processes in Physics and Chemistry. North-Holland, Amsterdam.

Wilson, R.E., Okubo, A., 1978. Longitudinal dispersion in a partially mixed estuary. Journal of Marine Research 36, 427–447.

Young, W.R., Rhines, P.B., Garrett, C.J.R., 1982. Shear-flow dispersion internal waves and horizontal mixing in the ocean. Journal of Physical Oceanography 12 (6), 515–527.